A New Manganese(II) Phosphate Templated by Ethylenediamine: $(C_2H_{10}N_2)[Mn_2(HPO_4)_3(H_2O)]$. Hydrothermal Synthesis, Crystal Structure, and Spectroscopic and Magnetic Properties

Jaione Escobal,[†] José L. Pizarro,[‡] José L. Mesa,[†] Luis Lezama,[†] Roger Olazcuaga,[§] María I. Arriortua,[‡] and Teófilo Rojo*[,†]

Departamentos de Química Inorgánica y Mineralogía-Petrología, Facultad de Ciencias, Universidad del País Vasco, Apdo. 644, E-48080 Bilbao, Spain and Institut de Chimie de la Matière Condenseé de Bordeaux, 33608 Pessac, France

Received June 22, 1999. Revised Manuscript Received September 13, 1999

A new manganese(II) phosphate templated by ethylenediamine, $(C_2H_{10}N_2)[Mn_2(HPO_4)_3(H_2O)]$, has been prepared by hydrothermal synthesis and characterized by single-crystal diffraction data and spectroscopic and magnetic techniques. The compound crystallizes in the monoclinic space group $P2_1/n$ with $a = 21.961(7)$, $b = 9.345(1)$, $c = 6.639(2)$ Å; $\beta = 91.06(2)°$; $V = 1362.3(6)$ Å^3; and $Z = 4$. The structure consists of anionic sheets of formula $[Mn_2(HPO_4)_3]^{2-}$, being the charge compensated by ethylendiammonium cations. The sheets are constructed by edge-sharing MnO_6 octahedra, MnO_5 trigonal bipyramids, and hydrogen phosphate tetrahedra. Within a layer, the edge-sharing octahedra and the trigonal bipyramids are linked in an alternating way, forming zigzag chains along the [001] direction. The ethylenediammonium cations and the water molecules are located in the interlayer space. The compound has been characterized by IR spectroscopy. A study of the compound by luminescence and diffuse reflectance spectroscopies is carried out. The Dq and Racah parameters have been calculated for Mn(II) ions in octahedral sites. The ESR spectra at different temperatures of the compound show isotropic signals, with a g value that remains unchanged with variation in temperature. The intensity and the line width of the ESR signals increase continuously from room temperature to 4.2 K. Magnetic measurements from room temperature to 1.8 K indicate the presence of antiferromagnetic interactions. A value of $J/k = -0.75$ K for the exchange parameter has been calculated by fitting the experimental magnetic data to a triangular lattice antiferromagnet of $S = {}^5/_2$ spins.

Introduction

Meso- and microporous materials are of great interest from both the industrial and academic point of view due to their catalytic, adsorbent, and ion-exchange properties.[1−3] In this way, phosphates of transition metals with open structures represent an interesting group of materials with potential catalytic applications. It has been recently shown that the incorporation of hydrogen-bonded organic molecules, especially diammonium cations, via hydrothermal synthesis is a very general method for the preparation of a large variety of novel organic−inorganic hybrid materials such as phosphates, phosphonates, and oxides with a large variety of transition metal ions.[4−10]

The first metallophosphates were prepared with the vanadium and molybdenum ions.[4,11] Recently, a number of works dealing with organically templated iron phosphates have evidenced a rich structural chemistry in this system.[12−15] In this way, some iron(III) and mixed-valence (Fe^{2+}/Fe^{3+}) iron phosphates with three-dimensional or layered structures together with isolated single chains are known.[12−18] In several cases, the magnetic and spectroscopic properties of these phases have been

* To whom all correspondence should be addressed. Telephone: 34-946012458. Fax: 34-944648500. E-mail: qiproapt@lg.ehu.es.
[†] Departamento de Química Inorgánica, Universidad del País Vasco.
[‡] Departamento Mineralogía-Petrología, Universidad del País Vasco.
[§] Institut de Chimie de la Matière Condenseé de Bordeaux.

(1) Davis, M. E.; Lobo, R. F. *Chem. Mater.* **1992**, *4*, 756.
(2) Breck, D. W. *Zeolite molecule sieves: structure, chemistry and use*; John Wiley & Sons: New York, 1974.
(3) Venuto, P. B. *Microporous Mater.* **1994**, *2*, 297.
(4) Haushalter, R.; Mundi, L. *Chem. Mater.* **1992**, *4*, 31.
(5) Soghomonian, V.; Chen, Q.; Haushalter, R.; Zubieta, J. *Chem. Mater.* **1993**, *5*, 1690.
(6) Kahn, M.; Lee, Y.; O'Connor, C.; Haushalter, R.; Zubieta, J. *J. Am. Chem. Soc.* **1994**, *116*, 4525.
(7) Zapf, P.; Rose, D.; Haushalter, R.; Zubieta, J. *J. Solid State Chem.* **1996**, *125*, 182.
(8) BeBord, J.; Haushalter, R.; Zubieta, J. *J. Solid State Chem.* **1996**, *125*, 270.
(9) Dhingra, S.; Haushalter, R. *J. Chem. Soc., Chem. Commun.* **1993**, *21*, 1665.
(10) Zhang, Y.; O'Connor, C.; Clearfield, A.; Haushalter, R. *Chem. Mater.* **1996**, *8*, 595.
(11) Khan, M. I.; Meyer, L. M.; Haushalter, R.; Schweitzer, A. L.; Zubieta, J.; Dye, J. L. *Chem. Mater.* **1996**, *8*, 43.
(12) Lii, K.-H.; Huang, Y.-F.; Zima, V.; Huang, C.-Y.; Lin, H.-M.; Jiang, Y.-C.; Liao, F.-L.; Wang, S.-L. *Chem. Mater.* **1998**, *10*, 2599.
(13) Cavellec, M.; Riou, D.; Greneche, J. M.; Ferey, G. *Inorg. Chem.* **1997**, *36*, 2181.
(14) DeBord, J. R. D.; Reiff, W. M.; Warren, C. J.; Haushalter, R.; Zubieta, J. *Chem. Mater.* **1997**, *9*, 1994.
(15) Lii, K. H.; Huang, Y. F. *J. Chem. Soc., Chem. Commun.* **1997**, 1311.

10.1021/cm9910815 CCC: $19.00
Published on Web 01/27/2000

also studied.[14,17] It can be concluded that the choice of organic guest molecules often has a deep influence on the final structure of the material. However, no relationship between the crystal structure of the compound and the nature of the organic molecule has been established.

An open-framework cobalt phosphate with ethylenediammonium cations containing a tetrahedrally coordinated cobalt(II) center[19] has been synthesized and studied. The synthesis of two cobalt(II) layered phosphates templated by 1,3-diaminopropane and 1,4-diaminobutane, respectively, has been also carried out.[8] Magnetic measurements of the 1,4-diaminobutane phase indicate the existence of a weak ferromagnetism from a canted interaction between the Co(II) ions present in the compound. In this work we report on the hydrothermal synthesis, crystal structure, and spectroscopic properties of a new manganese(II) phosphate templated by ethylenediammonium cations, $(C_2H_{10}N_2)[Mn_2(HPO_4)_3(H_2O)]$. The magnetic behavior of this compound has been also studied, showing the existence of antiferromagnetic interactions. As far as we are aware, this compound is the first manganese(II) phosphate templated by ethylenediamine.

Experimental Section

Synthesis and Characterization. $(C_2H_{10}N_2)[Mn_2(HPO_4)_3(H_2O)]$ was prepared from reaction mixtures of H_3PO_4 (3.75 mmol), ethylenediamine (3.75 mmol), and $MnCl_2{\cdot}4H_2O$ (0.75 mmol), in a mixture of ~15 mL of water and 1-butanol (volume ratio 1:2). The initial pH of the reaction mixture was ~9. The synthesis was carried out in a poly(tetrafluoroethylene)-lined stainless steel container under autogenous pressure, filled to ~75% volume capacity and all reactants were stirred briefly before heating. The reaction mixture was heated at 170 °C for 6 days, followed by slow cooling to room temperature. The pH of the reaction decreased up to ~5. The resulting product was filtered off, washed with ether, and dried in air. Light-pink plate aggregated crystals appeared in the preparation. The metal ion and phosphorus contents were confirmed by inductively coupled plasma atomic emission spectroscopy (ICP-AES) analysis. C,H,N-elemental analysis was carried out. Found: Mn, 22.7; P, 19.1; C, 4.9; H, 2.8; N, 5.7. $(C_2H_{10}N_2)[Mn_2(HPO_4)_3(H_2O)]$ requires Mn, 23.0; P, 19.4; C, 5.0; H, 3.1; N, 5.9. The density was measured by flotation in a mixture of $CHBr_3/CCl_4$. The obtained value was 2.3(2) g cm^{-3}. The decomposition curve obtained from the thermogravimetric study reveals a weight loss (~4%) between 100 and 300 °C that might be assigned to the water molecule present in the compound (calcd 3.9%). At temperatures above 300 °C, thermal decomposition of ethylenediamine occurs (~13%; calcd 13.4%). The X-ray diffraction spectrum of the residue obtained from the thermogravimetric analysis shows the presence of amorphous products, together with several peaks which can be assigned to the manganese pyrophosphate.

Single-Crystal X-ray Diffraction. The single-crystal used for the X-ray diffraction study was a fragment of a crystalline aggregate obtained in the synthesis with dimensions 0.22 × 0.20 × 0.04 mm. Diffraction data were collected at room temperature on an Enraf-Nonius CAD4 automated diffractometer using graphite-monochromated Mo Kα. Details of crystal data, intensity collection and some features of the structure refinement are reported in Table 1. Lattice constants were obtained by a least-squares refinement of the setting angles of 25 reflections in the range 8° < θ < 11°. Intensities and angular positions of two standard reflections were measured every hour and showed neither decrease nor misalignment during data collection.

Table 1. Crystal Data, Details of Data Collection, and Structure Refinement for the $(C_2H_{10}N_2)[Mn_2(HPO_4)_3(H_2O)]$ Phosphate

formula	$C_2H_{15}N_2O_{12}P_3Mn_2$
MW, g mol^{-1}	461.8
crystal system	monoclinic
space group	$P2_1/n$ (no. 14)
a, Å	21.961(7)
b, Å	9.345(1)
c, Å	6.639(2)
β, deg	91.06(2)
V, Å^3	1362.3(6)
Z	4
ρ_{calcd}, g cm^{-3}	2.330
F(000)	960
T, K	293
radiation, λ(Mo Kα), Å	0.71073
μ (Mo Kα), mm^{-1}	2.280
limiting indices	$-28 < h < 28, 0 < k < 11, 0 < l < 8$
R [$I > 2\sigma(I)$]	R1 = 0.097; wR2 = 0.218[a]
R [all data]	R1 = 0.130; wR2 = 0.241[a]
goodness of fit	1.037

[a] $R1 = [\sum(|F_o| - |F_c|)]/\sum|F_o|$; $wR2 = [\sum[w(|F_o|^2 - |F_c|^2)^2]/\sum[w(|F_o|^2)^2]]^{1/2}$; $w = 1/[\sigma^2|F_o|^2 + (xp)^2 + yp]$; where $p = [|F_o|^2 + 2|F_c|^2]/3$; $x = 0.0693$; $y = 49.01$.

A total of 3180 reflections were measured in the range 1° ≤ θ ≤ 27°. A total 2926 reflections were independent, applying the criterion $I > 2\sigma(I)$. Correction for Lorentz and polarization effects were done and also for absorption with the empirical ψ scan method[20] by using the XRAYACS program.[21] Direct methods (SHELXS 97)[22] were employed to solve the structure. The metal ion and the phosphorus atoms were first located. The oxygen, nitrogen, and carbon atoms were found in difference Fourier maps. The Mn(2) and Mn(3) ions are located in a special position with occupancy factors of 0.5 for each metallic ion. The structure was refined by the full-matrix least-squares method based on F^2, using the SHELXL 97 computer program.[23] The scattering factors were taken from ref 24. All non-hydrogen atoms were assigned anisotropic thermal parameters. Hydrogen atoms were geometrically placed, except for the water molecules which were not located. The final R factors were R1 = 0.097 [wR2 = 0.218]. Maximum and minimum peaks in final difference synthesis were 3.127 and −1.773 e Å^{-3} [near to the Mn(II) ions]. The final atomic positional parameters have been deposited at the Cambridge Crystallographic Data Centre. All drawings were made using ATOMS program.[25] Bond distances and angles are given in Table 2.

Physicochemical Characterization Techniques. C,H,N-elemental analysis was carried out with a Perkin-Elmer Model 240 automatic analyzer. Thermogravimetric measurements were performed in a Perkin-Elmer system 7 DSC-TGA instrument. A crucible containing ~20 mg of sample was heated at 5 °C min^{-1} under dry nitrogen atmosphere in the temperature

(16) Zima, V.; Lii, K.-H.; Nguyen, N.; Ducouret, A. *Chem. Mater.* **1998**, *10*, 1914.
(17) DeBord, J.; Reiff, W.; Haushalter, R.; Zubieta, J. *J. Solid State Chem.* **1996**, 125, 186.
(18) Lii, K.-H.; Huang, Y.-F. *J. Chem. Soc., Dalton Trans.* **1997**, 2221.
(19) Chen, J.; Jones, R. H.; Natarajan, S.; Hursthouse, M. B.; Thomas, J. M. *Angew. Chem., Int. Ed. Engl.* **1994**, *33*, 639.
(20) North, A. C. T.; Philips, D. C.; Mathews, F. S. *Acta Crystallogr.* **1968**, *A24*, 351.
(21) Chandrasekaran, A. XRAYACS: *Program for single-crystal X-ray data corrections*; Chemistry Department, University of Massachusetts: Amherst, MA, 1998.
(22) Sheldrick, G. M. SHELXS 97: *Program for the solution of crystal structures*; University of Göttingen: Göttingen, Germany, 1997.
(23) Sheldrick, G. M. SHELXL 97: *Program for the refinement of crystal structures*; University of Göttingen: Göttingen, Germany, 1997.
(24) *International tables for X-ray crystallography*; Kynoch Press: Birmingham, England, 1974; Vol. IV, p 99.
(25) Dowty, E. ATOMS: *A computer program for displaying atomic structures*; Shape Software: 521 Hidden Valley Road, Kingsport, TN, 1993.

Table 2. Bond Distances (Å) and Angles (deg) for $(C_2H_{10}N_2)[Mn_2(HPO_4)_3(H_2O)]$ (esd in parentheses)[a]

Bond Distances (Å)					
$Mn(1)O_5$ trigonal bipyramid		$Mn(2)O_6$ octahedron		$Mn(3)O_6$ octahedron	
Mn(1)−O(4)	2.129(7)	Mn(2)−O(3)/O(3)^{i}	2.228(7)	Mn(3)−O(3)/O(3)^{ii}	2.201(7)
Mn(1)−O(5)	2.267(7)	Mn(2)−O(6)/O(6)^{i}	2.177(6)	Mn(3)−O(5)/O(5)^{ii}	2.169(5)
Mn(1)−O(6)	2.228(7)	Mn(2)−O(10)/O(10)^{i}	2.158(7)	Mn(3)−O(10)^{iii}/O(10)^{i}	2.241(7)
Mn(1)−O(7)	2.041(8)				
Mn(1)−O(11)	2.119(7)				
$P(1)O_4$ tetrahedron		$P(2)O_4$ tetrahedron		$P(3)O_4$ tetrahedron	
P(1)−O(1)	1.514(8)	P(2)−O(5)	1.483(7)	P(3)−O(9)	1.500(8)
P(1)−O(2)	1.554(9)	P(2)−O(6)^{iii}	1.528(7)	P(3)−O(10)	1.542(7)
P(1)−O(3)	1.530(7)	P(2)−O(7)^{iv}	1.474(8)	P(3)−O(11)^{i}	1.541(7)
P(1)−O(4)	1.510(7)	P(2)−O(8)	1.600(9)	P(3)−O(12)	1.558(8)
		$(H_3N(CH_2)_2NH_3)^{2+}$			
N(1)−C(1)	1.52(2)	N(2)−C(2)	1.51(2)	C(1)−C(2)	1.45(2)
Bond Angles (deg)					
$Mn(1)O_5$ trigonal bipyramid		$Mn(2)O_6$ octahedron		$Mn(3)O_6$ octahedron	
O(4)−Mn(1)−O(11)	170.6(3)	O(10)−Mn(2)−O(10)^{i}	180.0(7)	O(5)−Mn(3)−O(5)^{ii}	180.0(5)
O(5)−Mn(1)−O(6)	133.1(2)	O(6)−Mn(2)−O(6)^{i}	180.0(5)	O(3)−Mn(3)−O(3)^{ii}	180.0(3)
O(5)−Mn(1)−O(7)	111.3(3)	O(3)−Mn(2)−O(3)^{i}	180.0(4)	O(10)−Mn(3)−O(10)^{i}	180(1)
O(6)−Mn(1)−O(7)	115.3(3)	O(10)−Mn(2)−O(6)^{i}	87.8(2)	O(5)−Mn(3)−O(3)	85.9(2) × 2
O(4)−Mn(1)−O(5)	88.9(3)	O(10)−Mn(2)−O(6)	92.2(2) × 2	O(5)−Mn(3)−O(3)^{ii}	94.1(2)
O(4)−Mn(1)−O(6)	87.5(3)	O(10)−Mn(2)−O(3)^{i}	78.2(2)	O(5)−Mn(3)−O(10)^{iii}	94.9(2) × 2
O(4)−Mn(1)−O(7)	88.6(3)	O(10)−Mn(2)−O(3)	101.7(2) × 2	O(5)−Mn(3)−O(10)^{i}	85.1(2)
O(11)−Mn(1)−O(5)	86.9(3)	O(10)^{i}−Mn(2)−O(6)	87.8(2)	O(5)^{ii}−Mn(3)−O(3)	94.1(2)
O(11)−Mn(1)−O(6)	89.2(3)	O(10)^{i}−Mn(2)−O(3)	78.2(2)	O(5)^{ii}−Mn(3)−O(10)^{iii}	85.1(2)
O(11)−Mn(1)−O(7)	100.7(3)	O(3)−Mn(2)−O(6)	87.1(2)	O(3)−Mn(3)−O(10)^{iii}	102.9(2)
		O(3)−Mn(2)−O(6)^{i}	92.9(2)	O(3)−Mn(3)−O(10)^{i}	77.1(2)
		O(6)−Mn(2)−O(3)^{i}	92.9(2)	O(10)^{iii}−Mn(3)−O(3)^{ii}	77.1(2)
		O(3)−Mn(2)−O(6)	87.1(2)	O(3)−Mn(3)−O(10)^{iii}	102.9(2)
$P(1)O_4$ tetrahedron		$P(2)O_4$ tetrahedron		$P(3)O_4$ tetrahedron	
O(1)−P(1)−O(2)	109.2(5)	O(5)−P(2)−O(7)^{iv}	117.2(4)	O(9)−P(3)−O(10)	112.3(4)
O(1)−P(1)−O(3)	111.0(4)	O(5)−P(2)−O(6)^{iii}	113.4(4)	O(9)−P(3)−O(12)	108.6(4)
O(1)−P(1)−O(4)	110.6(4)	O(5)−P(2)−O(8)	104.9(4)	O(9)−P(3)−O(11)^{i}	110.5(4)
O(2)−P(1)−O(3)	109.5(4)	O(6)^{iii}−P(2)−O(7)^{iv}	110.6(4)	O(10)−P(3)−O(12)	108.9(4)
O(2)−P(1)−O(4)	105.8(4)	O(8)−P(2)−O(6)^{iii}	105.6(4)	O(10)−P(3)−O(11)^{i}	110.5(4)
O(3)−P(1)−O(4)	110.6(4)	O(8)−P(2)−O(7)^{iv}	103.8(5)	O(12)−P(3)−O(11)^{i}	105.7(4)
		$(H_3N(CH_2)_2NH_3)^{2+}$			
N(1)−C(1)−C(2)	111(1)	C(1)−C(2)−N(2)	112(1)		

[a] Symmetry codes: i, $-x$, $-y+2$, $-z$; ii, $-x$, $-y+2$,$-z+1$; iii, x, y, $z+1$; iv, $-x$,$-y+1$, $-z+1$.

range 30−800 °C. The IR spectrum (KBr pellet) was obtained with a Nicolet FT-IR 740 spectrophotometer in the 400−4000 cm^{-1} range. Luminescence measurements were carried out in a Spectrofluorometer Fluorolog-2 SPEX 1680, model F212I at 4.2 K. The excitation source was a high-pressure xenon lamp emitting between 200 and 1200 nm. The diffuse reflectance spectrum was registered at room temperature on a Cary 2415 spectrometer in the 210−2000 nm range. A Bruker ESP 300 spectrometer was used to record the ESR polycrystalline spectra from room temperature to 4.2 K. The temperature was stabilized by an Oxford Instrument (ITC 4) regulator. The magnetic field was measured with a Bruker BNM 200 gaussmeter, and the frequency inside the cavity was determined using a Hewlett-Packard 5352B microwave frequency counter. Magnetic measurements of powdered sample were performed in the temperature range 1.8−300 K, using a Quantum Design MPMS-7 SQUID magnetometer. The magnetic field was ∼0.1 T, a value lying within the range of linear dependence of magnetization vs magnetic field even at 1.8 K.

Results and Discussion

Crystal Structure. The structure consists of anionic sheets of formula $[Mn_2(HPO_4)_3]^{2-}$, in the *bc* plane, which charge is compensated by ethylenediammonium cations (Figure 1a). The sheets are constructed from MnO_6 octahedra and MnO_5 trigonal bipyramids which are joined by bridging hydrogen phosphate tetrahedra (Figure 1b). Within a layer, the Mn(2),(3)O_{10} edge-sharing octahedra and one $Mn(1)O_5$ trigonal bipyramid, which is linked in alternating way to two different MnO_6 octahedra, form zigzag chains along the [001] direction. $Mn(1)O_5$ trigonal bipyramids, from two different chains, are linked via $P(2)O_4$ tetrahedra, delimiting four-sided windows. The ethylenediammonium cations and the water molecules are located in the interlayer space of the $[Mn_2(HPO_4)_3]^{2-}$ sheets.

A remarkable structural feature of this compound is the presence of the Mn_3O_{13} cluster formed from two MnO_6 edge-sharing octahedra and one MnO_5 trigonal bipyramid, which shares two oxygen atoms from different MnO_6 octahedra (Figure 1c). In the MnO_5 trigonal bipyramids, the Mn(1) ion is bonded in equatorial positions to the O(5), O(6), and O(7) atoms, belonging to the $P(2)O_4$ tetrahedra, with bond distances of 2.267(7), 2.228(7), and 2.041(8) Å, respectively. The axial positions are occupied by the O(4) and O(11) atoms, belonging to the $P(1)O_4$ and $P(3)O_4$ groups, respectively, with bond distances of 2.129(7) and 2.119(7) Å. The *equatorial* O−Mn(1)−O angles range from 111.3(3)° to 133.1(2)°, whereas the O_{ap}−Mn(1)−O_{eq} angles range from 86.9(3)° to 100.7(3)°. The *trans*-O−Mn(1)−O angle deviates from the ideal value by ∼10°. The distortion of this coordination polyhedron from trigonal bipyramid ($\Delta = 0$) toward a regular square pyramid ($\Delta = 1$), calculated by quantification of the Muetterties and Guggenberger description,[26,27] is $\Delta = 0.36$, which indicates a topology near to trigonal bipyramid. The MnO_6 octahedra share the O(3)−O(10) edge from the $P(1)O_4$

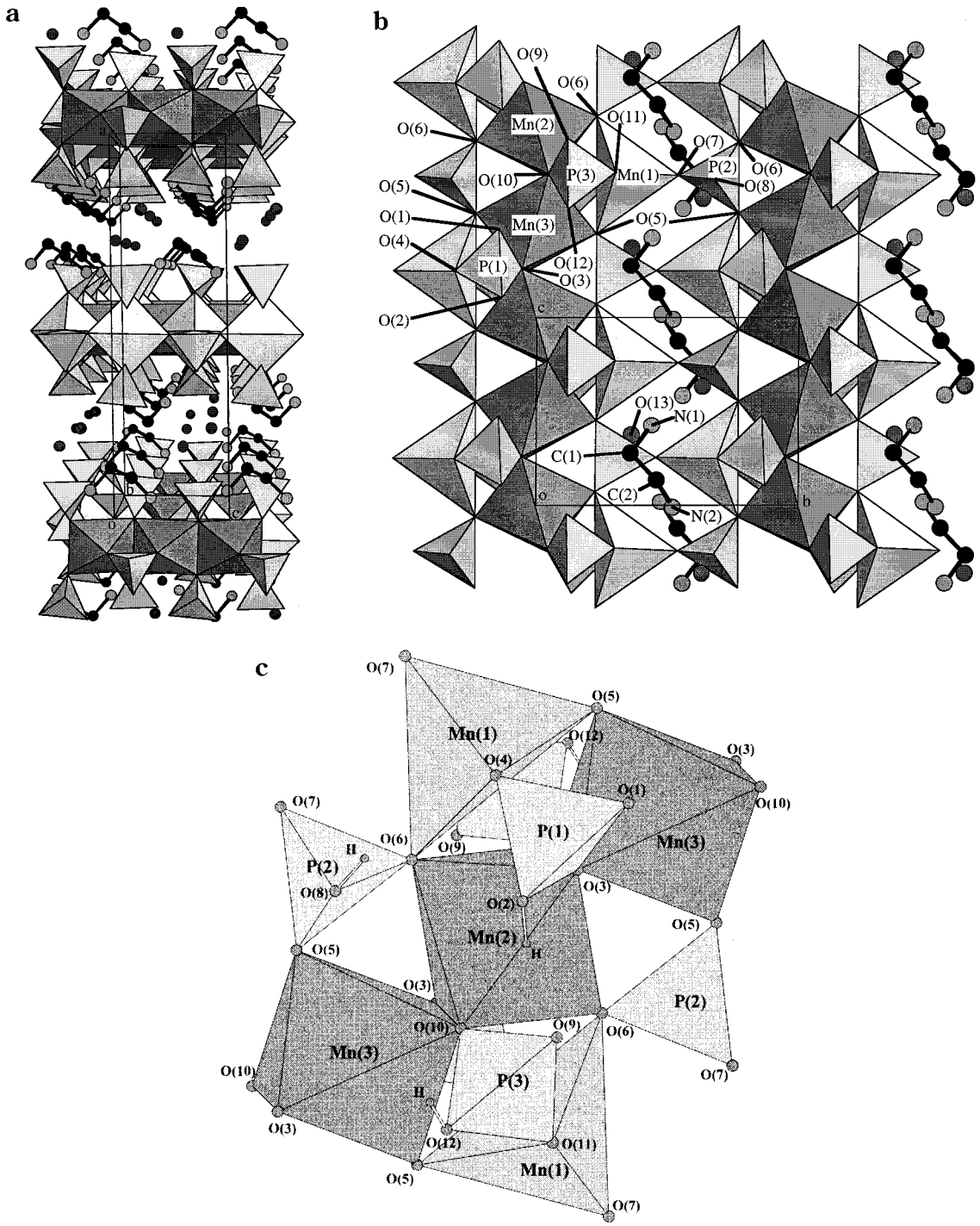

Figure 1. (a) Polyhedral view of $(C_2H_{10}N_2)[Mn_2(HPO_4)_3(H_2O)]$, showing the layered structure; (b) polyhedral representation of $(C_2H_{10}N_2)[Mn_2(HPO_4)_3(H_2O)]$ in the *bc* plane, showing a layer with detailed labeling of the atoms; and (c) view of the Mn_3O_{13} cluster of $(C_2H_{10}N_2)[Mn_2(HPO_4)_3(H_2O)]$.

and $P(3)O_4$ phosphates with bond distances Mn(2)−O(3) and Mn(2)−O(10) of 2.228(7) and 2.158(7) Å, respectively and Mn(3)−O(3) and Mn(3)−O(10) of 2.201(7) and 2.241(7) Å, respectively. The other two Mn(2)−O(6) and Mn(3)−O(5) bond lengths are provided by $P(2)O_4$ tetrahedra with values of 2.177(6) and 2.169(5) Å, respectively. The *cis*-O−Mn−O angles range from 78.2(2)° to 101.7(2)° for $Mn(2)O_6$ octahedron and from 77.1(2)° to 102.9(2)° for $Mn(3)O_6$ octahedron. The *trans*-O−Mn−O angles are practically of 180°, in both octahedral polyhedra due to the special position occupied by the Mn(II) ions. The distortions of these polyhedra, from an octahedron ($\Delta = 0$) to a trigonal prism ($\Delta = 1$),[26,28] are $\Delta = 0.065$ and 0.060 for $Mn(2)O_6$ and $Mn(3)O_6$ polyhedra, respectively, which indicate a topology near to octahedron.

(26) Muetterties, E. L.; Guggenberger, L. J. *J. Am. Chem. Soc.* **1974**, *96*, 1748.

(27) Mesa, J. L.; Arriortua, M. I.; Lezama, L.; Pizarro, J. L.; Rojo, T.; Beltrán, D. *Polyhedron* **1988**, *7*, 1383.

(28) Cortés, R.; Arriortua, M. I.; Rojo, T.; Solans, X.; Beltran, D. *Polyhedron* **1986**, *5*, 1987.

The HPO_4 tetrahedra are practically regular, with mean bond distances P−O of 1.52(3) Å. The P(1)−O(2), P(2)−O(8), and P(3)−O(12) are hydrogen phosphate groups, with bond distances slightly longer than those observed for the other P−O distances. The O−P−O angles are in the range from 103.8(5)° to 117.2(4)°. The ethylendiammonium cation establishes hydrogen bonds with oxygen atoms belonging to hydrogen phosphate anions. The bond lengths range from 2.75(1) to 3.15(1) Å. Furthermore, the water molecule forms hydrogen bonds of 2.80(1) and 2.88(1) Å with N(1) and N(2) atoms of the ethylendiammonium cation, respectively. Three P−O···O(w) hydrogen bonds with the O(1), O(8), and O(9) atoms and distances of 2.78(1), 2.77(1), and 3.00(1) Å, respectively, are also observed.

IR, Luminescence, and UV−Vis Spectroscopy. The IR spectrum of $(C_2H_{10}N_2)[Mn_2(HPO_4)_3(H_2O)]$ shows bands corresponding to the vibrations of the water, ethylenediammonium cations, and hydrogen phosphate anions. The strong band centered at 3385 cm^{-1} corresponds to the stretching mode of the water molecule. The bending mode of this molecule can be observed at ∼1625 cm^{-1}. The stretching mode of the $(NH_3)^+$ group, in the ethylenediammonium cation, appears at 3095 cm^{-1}. The band near to 1575 cm^{-1} can be assigned to the $(NH_3)^+$ bending vibration. This band is indicative of the presence of the ethylenediamine molecule in its protonated form,[29,30] in good agreement with the structural results. The bending modes of the $-CH_2-$ groups in the ethylenediammonium appear in the 1400−1200 cm^{-1} range. Four different groups of bands can be attributed to the vibrational modes of the $(HPO_4)^{2-}$ anions present in the compound.[31] The asymmetric ν_{as}(P−O) stretching mode appears at 1125, 1045, and 970. The symmetric ν_s(P−O) stretch is detected at 680 cm^{-1}. The asymmetric deformation vibrations [δ_{as}(O−P−O)] are observed at 560, 555, and 465 cm^{-1}. Finally, the weak band observed at about 1470 cm^{-1} can be assigned to the bending mode of the H−OP group, in good agreement with the structural results.

Luminescence measurements of the Mn(II) ion in $(C_2H_{10}N_2)[Mn_2(HPO_4)_3(H_2O)]$ have been carried out at 4.2 K. Figure 2a shows the emission spectrum of the compound obtained under a 356 nm excitation. It exhibits a unique red emission peaking at 652 nm which is characteristic of an octahedral environment for the Mn(II) (d^5) ions. The excitation spectrum (λ_{em} = 650 nm) (Figure 2b) reveals a spectral distribution of bands corresponding to the excited levels of Mn(II) [$^4T_1(^4G)$, 551 nm; $^4T_2(^4G)$, 432 nm; $^4A_1,^4E(^4G)$, 408 nm; $^4T_2(^4D)$, 369 nm; $^4E(^4D)$, 356 nm]. These values are in accord with those generally observed for Mn(II) in an octahedral site.[32,33] No emission corresponding to Mn(II) ions in a trigonal bipyramid environment was observed. The diffuse reflectance spectrum of this compound exhibits several very weak spin-forbidden d−d bands, at ca. 355, 365, 405, 425, and 530 nm. The position of these bands

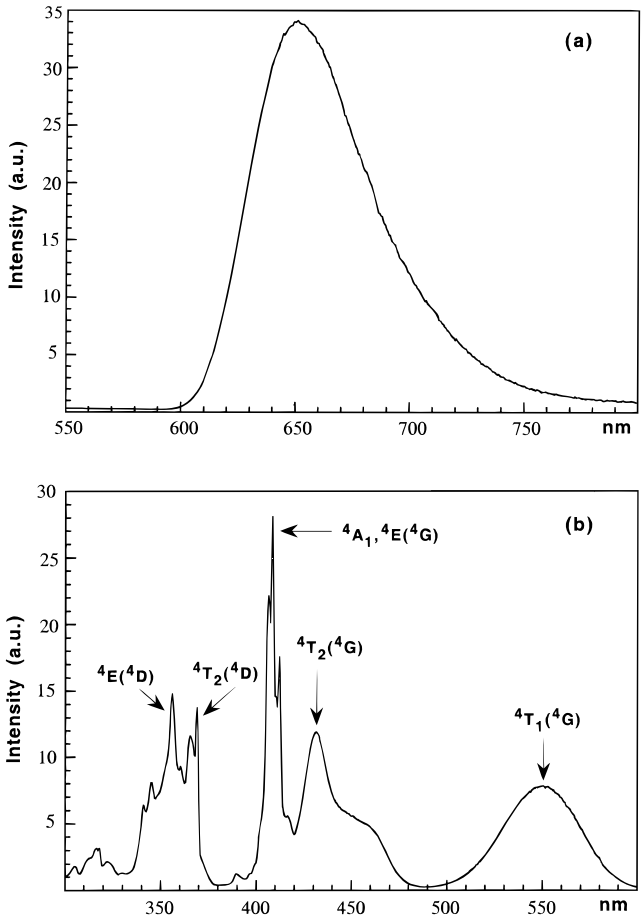

Figure 2. (a) Emission spectrum (λ_{exc} = 356 nm) and (b) excitation spectrum (λ_{em} = 650 nm) of $(C_2H_{10}N_2)[Mn_2(HPO_4)_3(H_2O)]$ at 4.2 K.

is similar to that obtained from the luminescence results and therefore can be assigned to the Mn(II) ions in an octahedral environment. Furthermore, the reflectance spectrum shows a band at ∼270 nm, which could be tentatively assigned to the more energetic transition $^6A'_1(S) \rightarrow {}^4E''(D)$ in a trigonal-bipyramid environment.[34]

Taking into account the results of the luminescence and diffuse reflectance spectroscopies, the Dq and Racah parameters have been calculated by fitting the experimental frequencies to an energy level diagram for octahedral d^5 high-spin system.[35] The values obtained are Dq = 945, B = 515, and C = 3865 cm^{-1}. These values are in the range usually found for octahedrally coordinated Mn(II) compounds.[36,37]

ESR and Magnetic Properties. ESR spectra of $(C_2H_{10}N_2)[Mn_2(HPO_4)_3(H_2O)]$ have been recorded on a powdered sample at X-band between 4.2 and 300 K and are shown in Figure 3a. The spectra remain essentially unchanged upon cooling the sample from 300 to 50 K. Below this temperature, however, the line width of the spectra increases rapidly. The spectra are isotropic with a g value of ∼2.011, which remains unchanged with variation in temperature. The temperature dependence of the intensity and the line width of the signals

(29) Gharbi, A.; Jouini, A.; Averbuch-Pouchot, M. T.; Durif, A. *J. Solid State Chem.* **1994**, *111*, 330.
(30) Dolphin, D.; Wick, A. E. *Tabulation of infrared spectral data*; John Wiley & Sons: New York, 1977.
(31) Nakamoto, K. *Infrared and raman spectra of inorganic and coordination compounds*; John Wiley & Sons: New York, 1997.
(32) Orgel, L. E. *J. Chem. Phys.* **1955**, *23*, 1004.
(33) Tanabe, Y.; Sugano, S. *J. Phys. Soc. Jpn.* **1954**, *9*, 753.
(34) Ciampoli, M.; Mengozzi, C. *Gazz. Chim. Ital.* **1974**, *104*, 1059.
(35) Lever, A. B. P. *Inorganic electronic spectroscopy*; Elsevier Science Publishers B.V.: Amsterdam, Netherlands, 1984.
(36) Lawson, K. E. *J. Chem. Phys.* **1966**, *44*, 4159.
(37) Escobal, J.; Mesa, J. L.; Pizarro, J. L.; Lezama, L.; Olazcuaga, R.; Rojo, T. *J. Mater. Chem.* **1999**, *9*, 2691.

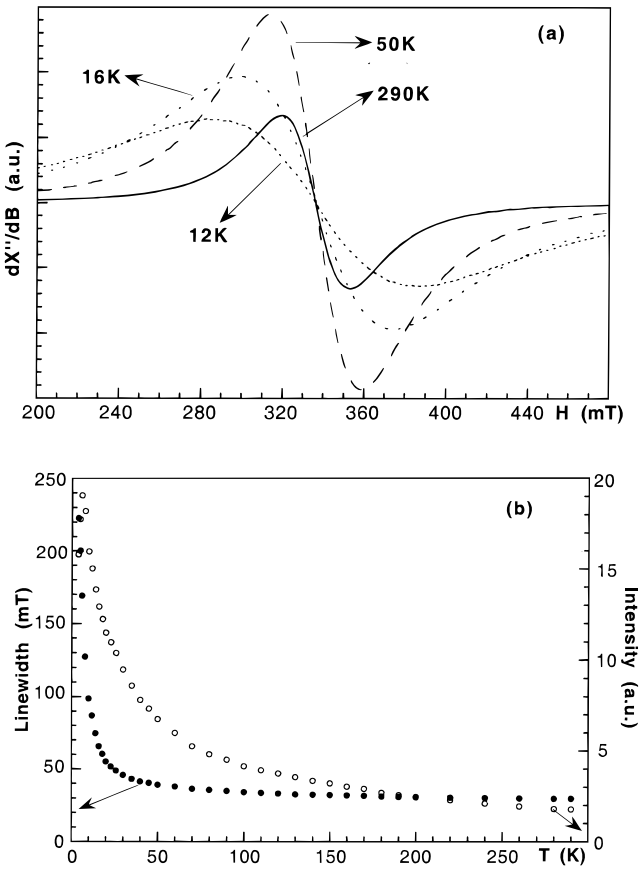

Figure 3. (a) Powder X-band ESR spectra of $(C_2H_{10}N_2)[Mn_2(HPO_4)_3(H_2O)]$, at different temperatures, and (b) temperature dependence of the intensity of the signal and the line width curves.

calculated by fitting the experimental spectra to Lorentzian curves are displayed in Figure 3b. The intensity of the signal increases in the temperature range studied and does not exhibit any substantial decrease at low temperatures. The weak diminution observed below 6 K is probably due to an effect of integration of the signals, caused by the long line width of the curves at low temperature. This behavior could be explained considering the compound as either a paramagnetic or an antiferromagnetic system in which the maximum in the magnetic susceptibility appears at temperatures lower than 4.2 K, the minimum temperature at which operates the ESR spectrometer used in the experiment. The line width of the ESR signal increases slightly from room temperature to ~50 K probably caused by a dipolar homogeneous broadening. When the temperature is further decreased the line width increases vigorously due to a strong spin correlation. These results are in good agreement with those observed for other magnetic systems, where the line width increases drastically when the temperature approximates to the critical one.[38−42]

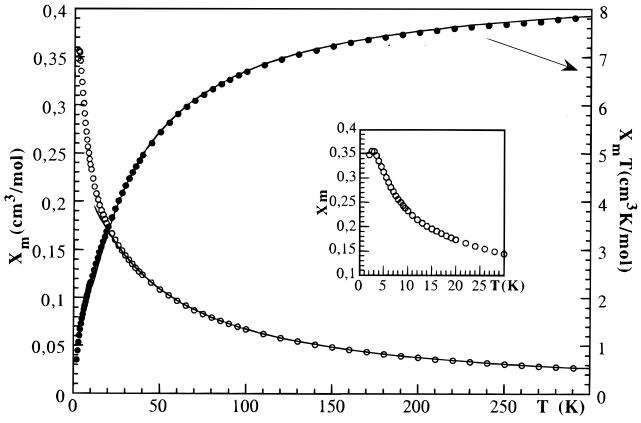

Figure 4. Thermal evolution of χ_m and $\chi_m T$ curves of the $(C_2H_{10}N_2)[Mn_2(HPO_4)_3(H_2O)]$ compound. The inset shows the maximum in the χ_m vs T curve. The solid lines show the fit of the χ_m and $\chi_m T$ experimental data to the triangular lattice antiferromagnet model.

Variable-temperature magnetic susceptibility measurements of $(C_2H_{10}N_2)[Mn_2(HPO_4)_3(H_2O)]$ have been carried out on a powdered sample in the range from 1.8 to 300 K. Plots of the χ_m and $\chi_m T$ vs T curves are shown in Figure 4. The thermal evolution of χ_m follows the Curie−Weiss law at temperatures >50 K, with C_m = 4.28 (cm^3 K)/mol and $\theta = -28.1$ K. At lower temperatures, the molar magnetic susceptibility increases with decreasing temperature and reaches a maximum at 2.5 K, indicating that a long magnetic order is established at this temperature (inset in Figure 4). This result together with the continuous decrease in the $\chi_m T$ vs T curve, from 7.924 μ_B at room temperature up to 2.361 μ_B at 1.8 K, is indicative of antiferromagnetic exchange couplings in the compound.

These results suggest the presence of a three-dimensional magnetic system formed by superexchange magnetic interactions through the hydrogen phosphate anions within the $[Mn_2(HPO_4)_3]^{2-}$ sheets and interlayer interactions probably with dipolar character. However, considering the structural features of this compound, in which the interlayer distance between the $[Mn_2(HPO_4)_3]^{2-}$ sheets is higher than ~10 Å, a three-dimensional magnetic model can be a priori disregarded for the analysis of the magnetic behavior. In the same way a classical regular square two-dimensional model can also be disregarded in the magnetic analysis due to the MnO_6 octahedra and MnO_5 trigonal bipyramids are forming zigzag chains within the layers. From the magnetic point of view, a more realistic approximation to the problem would be to study the system using a triangular lattice antiferromagnet model of $S = {}^5/_2$ spin. Three superexchange magnetic pathways can be considered (see Figure 5). Two of them, J_1 and J_2, are formed by zigzag pathways involving the Mn(2)−Mn(1)−Mn(3) cations with angles Mn(2)−O(6)−Mn(1) and Mn(1)−O(5)−Mn(3) at ~102 and ~104°, respectively. The third pathway along the chains, J_3, between edge-sharing octahedra, involves the Mn(2)−Mn(3)−Mn(2) cations with two similar bond angles Mn(2)−O(3)−Mn(3) and Mn(2)−O(10)−Mn(3) at ~97 and ~98°, respectively (see Figure 5a). On the basis of this situation and considering that $J_1 \approx J_2 \approx J_3$ (Figure 5b), the experimental magnetic data (Figure 4) were fitted

(38) Wijn, H. W.; Walker, L. R.; Daris, J. L.; Guggenheim, H. *J. Solid Sate Commun.* **1972,** *11*, 803.
(39) Richards, P. M.; Salamon, M. B. *Phys. Rev. B* **1974**, *9*, 32.
(40) Escuer, A.; Vicente, R.; Goher, M. A. S.; Mautner, F. *Inorg. Chem.* **1995**, *34*, 5707.
(41) Bencini, A.; Gatteschi, D. *EPR of exchange coupled systems*; Springer-Verlag: Berlin, 1990.
(42) Cheung, T. T. P.; Soos, Z. G.; Dietz, R. E.; Merrit, F. R. *Phys. Rev. B* **1978**, *17*, 1266.

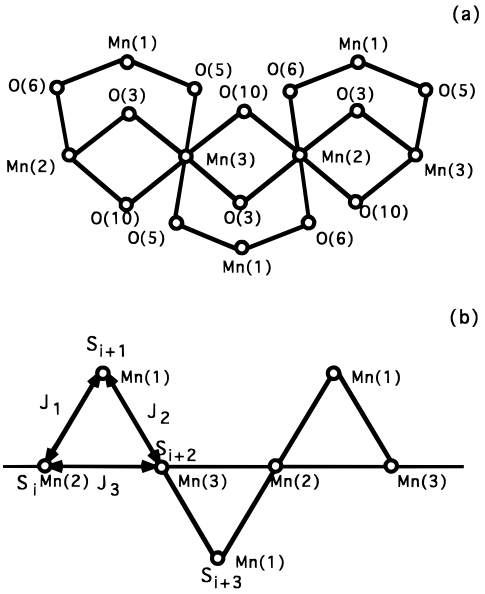

Figure 5. Sketch of the exchange pathways corresponding to first neighbor interactions, showing (a) the bond angles involved in the magnetic exchange and (b) the different *J*-exchange parameters, J_1 and J_2, zigzag pathways, and J_3, along the chains of $S = {}^5/_2$ spins.

to the expression derived by Rushbrooke and Wood:[43]

$$\chi_m = (35N\beta^2g^2/12kT)(1 + 35x + 221.667x^2 - 1909.83x^3 + 6156.92x^4 + 84395.9x^5 - 1522000x^6)^{-1} \quad (1)$$

where, $x = |J|/kT$, k is the Boltzmann constant, N is Avogadro's number, and β is the Bohr magneton. The best fit to the χ_m and $\chi_m T$ data (solid lines in Figure 4) is obtained for a value of the magnetic exchange J parameter of $J/k = -0.75$ K and $g = 1.977$. The theoretical model proposed in the eq 1 does not fit exactly the magnetic behavior of this compound below 7 K. Therefore, the obtained J exchange parameter must be considered as an approximate result. Attempts performed to fit the data considering an exchange parameter between the sheets, J', did not give an improvement of the results, which confirms that the main magnetic interactions occur within the $[Mn_2(HPO_4)_3]^{2-}$ sheets.

(43) Rushbrooke, G. S.; Wood, P. J. *Mol. Phys.* **1958**, *1*, 257.

Concluding Remarks

The first manganese(II) phosphate templated by ethylenediamine with formula $(C_2H_{10}N_2)[Mn_2(HPO_4)_3(H_2O)]$ has been prepared under hydrothermal conditions. Its crystal structure has been resolved by X-ray single-crystal data diffraction. The crystal structure of this manganese−phosphate consists of inorganic sheets of composition $[Mn_2(HPO_4)_3]^{2-}$, with ethylenediammonium cations located in the interlayer region. Within the sheets, the Mn(II) ions exhibit two different environments, octahedron and trigonal bipyramid. These polyhedra are linked by hydrogen phosphate anions, givins rise to zigzag chains along the [001] direction. The Dq and Racah (B and C) parameters have been calculated, and they are in the range usually found for Mn(II) ions in octahedral sites. The ESR spectra are isotropic, with a g value which remains unchanged from room temperature to 4.2 K. The intensity and the line width of the ESR signals increase in the range 300 to 4.2 K. Magnetic measurements up to 1.8 K indicate antiferromagnetic exchange couplings. The magnetic exchange parameter, $J/k = -0.75$ K, has been calculated considering the compound as a triangular lattice antiferromagnet with only an interaction pathway.

Acknowledgment. This work was financially supported by the Ministerio de Educación y Ciencia and Universidad del País Vasco/EHU (grants PB97-0640 and 169.310-EB149/98, respectively), which we gratefully acknowledge. We thank F. Guillen (I.C.M.C.B.; Pessac, France) for luminescence measurements at low temperature. J.E. thanks the UPV/EHU for a doctoral fellowship.

Supporting Information Available: X-ray crystal data and structure factors for $(C_2H_{10}N_2)[Mn_2(HPO_4)_3(H_2O)]$. This material is available free of charge via the Internet at http://pubs.acs.org.

CM9910815